Available online at www.sciencedirect.com

ScienceDirect

Procedia CIRP 95 (2020) 220–225

www.elsevier.com/locate/procedia

20th CIRP Conference on Electro Physical and Chemical Machining (ISEM 2020)

The Tool Electrode Wear and Gap Fluid Field Simulation Analysis in Micro-EDM Drilling of Micro-hole Array

Huan Liu, Jicheng Bai*

School of Mechatronics Engineering, Harbin Institute of Technology, Harbin 150001, China

* Corresponding author. Tel.: +86-0451-86402636; fax: +86-0451-86402636. *E-mail address:* jichengbai@hit.edu.cn

Abstract

With the micro-hole array structure has been widely used in industrial areas, such as inkjet printer nozzle, oil nozzle, spinneret and so on, its processing accuracy significantly affects the performance of the product. In the machining of micro-hole array by micro-EDM drilling, unavoidable tool electrode wear and frequent occurrence of abnormal discharges such as short circuit and secondary discharge caused by the difficulty in removing discharge debris are the main factors affecting machining geometric and dimensional accuracy. In this study, the flow velocity simulation analysis of working fluid playing a crucial role in the flushing of discharge debris and the experimental study on the axial wear of tool electrode are explored in order to ensure the machining accuracy of micro-hole array. By changing the parameters of tool electrode diameter and machining depth in the fluid field simulation analysis, the gap velocity distribution under different depth-diameter ratios is obtained. Simulation results show that the gap flow velocity decreases with depth-diameter ratios increasing. For different depth-diameter ratios in the micro-hole array processing, the tip morphology evolution and the wear of tool electrode are considered, which show that the electrode tip morphology tends to be stable and the axial wear of the tool electrode could be compensated evenly. In addition, the characteristics of tool electrode axial wear are explained based on the simulation results of gap flow field, which verifies the effectiveness of the flow field simulation and provides a reference for formulating electrode wear compensation strategy and improving machining accuracy to some extent.

Keywords: Micro-EDM drilling; Micro-hole array; Fluid field simulation; Tool electrode wear

1. Introduction

With the rapid development of industrial technology, a variety of micro-structure, fine parts, micro-transmission agencies have been widely used in the aerospace, electronic communications, medical equipment, printing equipment and other industrial fields [1-3]. Micro electrical discharge machining (micro-EDM) with the characteristic of noncontact machining is an effective method for machining conductive materials regardless their hardness and toughness, and shows good machining capacity for new difficult-to-cut materials. With the continuous improvement of basic theory [4, 5] and machining performance [6, 7], micro-EDM has become one of the most common methods for micro-structure machining.

In micro-EDM, there is no effective detection method for the direct effect of working fluid in the machining gap on the debris because of the so small machining gap. The commonly used method is to establish the gap flow field simulation to simulate the distribution of flow field during machining. Zhu et al. [8] investigated the velocity distribution of the gap flow field in micro-EDM with a rotating electrode, finding that appropriately increasing the flow rate and reducing the flushing angle could improve the quality of the micro-holes. Kliuev et al. [9] investigated the influence of drilling conditions on pressure drop and dielectric flow during EDM drilling by numerical simulation and analysed turbulences, pressure and velocity distribution, finding that the diameter and configuration of internal flushing channel had a significant effect on the flushing speed and efficiency of debris particle removal especially for small diameter electrodes and complex multi-channel electrodes. Maradia et al. [10] exploited optimal flushing conditions of complex-shaped slot EDM machining by fluid dynamics simulation, inferring that the flushing efficiency in an even hole and an overlapping hole condition was not

2212-8271
10.1016/j.procir.2020.02.278

homogeneous along all directions and further deteriorated the erosion efficiency. Bozdana and Al-Karkhi [11] discussed the numerical investigation on the effectiveness of electrode geometry on flushing and debris removal in EDM, indicating that the overall performance of side-cut electrode was superior due to improved erosion rates and flushing capabilities. Feng et al. [12] researched the velocity field of gap medium and the distribution of the debris at different speeds in EDM with high-speed tool electrode rotation, and pointed out that increasing the rotating speed of the tool electrode brings higher removal rate and lower electrode wear and taper of the hole. The above research progress shows that the remarkable achievements of gap fluid field simulation are mainly focused on the factors affecting the flow velocity in the machining gap and the effective measures improving the debris discharge. However, the flow field distribution in the machining gap under different depth-diameter ratios and its influence on electrode wear are still challenging tasks.

In the machining process of micro-hole array, electrode wear has an important impact on the dimensional accuracy and its consistency accuracy of micro-holes. In order to improve the effect of electrode wear on machining accuracy, a number of approaches have been applied on electrode wear. Bissacco et al. [13] found that the size of spark discharge energy was an important factor affecting the electrode wear, while the shape of discharge pulse had little correlation with the electrode wear. Kruth and Lauwers [14] investigated the rules of electrode wear for different machining objects and methods, finding that the stability of the machining conditions and the feeding means also had effect on electrode wear. The electrode wear of piezoelectric self-adaptive micro-EDM method was explored by Zhang et al. [15], discovering that the method could effectively reduce the occurrence of abnormal discharges, thereby decreasing the abnormal electrode wear. In summary, great progress has been made in the influencing factors and improvement measures of electrode wear. However, it is still much room for further research on the evolution rule of electrode tip morphology and the characteristic of tool electrode wear at different depth-diameter ratios in the micro-hole array processing.

In this paper, the flow velocity distribution of gap flow field is firstly obtained by simulation analysis under different depth-diameter ratios. In order to get the evolution rule of electrode tip morphology and the characteristic of tool electrode wear, experimental research on micro-hole array EDM machining under different depth-diameter ratios is carried out. Moreover, the simulation results of gap flow field and the experimental results of electrode wear characteristics under different depth-diameter ratios are compared and analysed to prove the validity of the simulation results and obtain the influence of the flow field distribution in the machining gap on the electrode wear.

Nomenclature

d	Tool electrode diameter (μm)
h	Machining depth (μm)
χ	Depth-diameter ratio
v_r	Tool electrode rotating velocity (rpm)
v_f	Inlet velocity of dielectric fluid (m/s)

2. Simulation of machining process

2.1. Principle of Micro-EDM

Micro-EDM is a nontraditional machining method which removes the material by rapid and repeated discharges between electrode and workpiece. Fig. 1 shows a schematic diagram of Micro-EDM. During the machining process of Micro-EDM, the tool electrode feed downwards while rotating at high velocity, and the working fluid with certain insulation strength is injected into the processing area from workpiece surface to facilitate the generation of pulsed spark discharge. At the same time, the working fluid takes away debris in the machining gap and dissipates the generated heat produced by spark discharge. After the workpiece is completely penetrated by the tool electrode, the process is finished, the shape of the tool electrode tip is observed and the tool electrode wear is calculated.

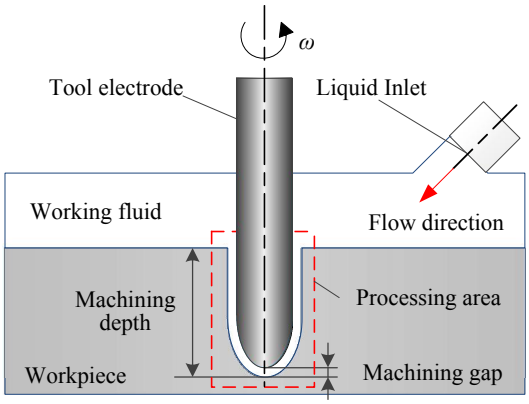

Fig. 1 Schematic diagram of micro-EDM

2.2. Selection of simulation parameters

As an important part of EDM, working fluid has an important impact on machining performance. In the micro-hole EDM machining, the processing of both the initial and the penetrate stages are better than the machining stage. In this paper, the flow velocity of the gap flow field in machining stage is mainly discussed.

This paper assumes that the deionized water working fluid has the following properties:

1. Deionized water is an incompressible continuous medium.
2. The electrical parameters do not change with time.
3. The size of the debris in the flow field is so small that it does not affect the flow field.
4. Deionized water is approximately maintained at constant temperature.

Based on the above assumptions, the continuity equation of the working fluid could be expressed as follows:

$$\frac{\partial V_x}{\partial x}+\frac{\partial V_y}{\partial y}+\frac{\partial V_z}{\partial z}=0 \tag{1}$$

The Navier-Stokes equation is simplified as follows:

$$\frac{\partial V_x}{\partial t}+(V_x\frac{\partial V_x}{\partial x}+V_y\frac{\partial V_x}{\partial y}+V_z\frac{\partial V_x}{\partial z})=F_x-\frac{1}{\rho}\frac{\partial P}{\partial x}+\nu(\frac{\partial^2 V_x}{\partial x^2}+\frac{\partial^2 V_x}{\partial y^2}+\frac{\partial^2 V_x}{\partial z^2}) \tag{2}$$

$$\frac{\partial V_y}{\partial t}+(V_x\frac{\partial V_y}{\partial x}+V_y\frac{\partial V_y}{\partial y}+V_z\frac{\partial V_z}{\partial z})=F_y-\frac{1}{\rho}\frac{\partial P}{\partial y}+\nu(\frac{\partial^2 V_y}{\partial x^2}+\frac{\partial^2 V_y}{\partial y^2}+\frac{\partial^2 V_y}{\partial z^2}) \quad (3)$$

$$\frac{\partial V_z}{\partial t}+(V_x\frac{\partial V_z}{\partial x}+V_y\frac{\partial V_z}{\partial y}+V_z\frac{\partial V_z}{\partial z})=F_z-\frac{1}{\rho}\frac{\partial P}{\partial x}+\nu(\frac{\partial^2 V_z}{\partial x^2}+\frac{\partial^2 V_z}{\partial y^2}+\frac{\partial^2 V_z}{\partial z^2}) \quad (4)$$

Where Vx、Vy、Vz and Fx、Fy、Fz represent the velocity component and the volume force component in the three directions of x、y、z in the coordinate system respectively, t is the time, ρ is the fluid density, v is the kinematic viscosity coefficient, and P is the fluid pressure.

For flow field simulation analysis ANSYS Fluent 18.0 software is used, while GAMBIT software is used to establish a three-dimensional geometric model of the working fluid field. As the small area between electrode and workpiece is the focus of the simulation study, a refined mesh is required. The liquid inlet is set as the velocity-inlet boundary. The electrode surface, the inner wall of micro-hole, and the upper surface of workpiece are set as wall boundaries (the electrode surface is a rotating wall boundary that can be set to different velocities). Other boundaries are the interface between the dielectric regions and the outside; these are set to pressure-outlet boundary conditions. The external condition is set at standard atmospheric pressure, and the hydrostatic pressure of the border is 0 Pa. The fluid is deionised water, the calculation model is a turbulence model, and k-ε is selected as the model solution. The parameters used in the calculations are listed in Table 1. Five groups of simulation conditions are designed in this paper. In order to research the effect of electrode diameter and machining depth on the experimental results, the machining depth of 100 μm, 200 μm, 300 μm are chosen, and the tool electrode diameters of 80 μm, 100 μm, 120 μm are selected. When the depth-diameter ratio is too small, the velocity variation of working fluid is not obvious, and when the depth-diameter ratio is too large, the hole is hard to penetrate. In addition, the tool electrode rotating velocity is set at 2000 rpm and the outlet velocity of working fluid is 10 m/s.

Table 1. Simulation parameters for the gap flow field analysis.

Group	d (μm)	h (μm)	χ	v_r (rpm)	v_f (m/s)
1	80	100	1	2000	10
2	80	200	2	2000	10
3	80	300	3	2000	10
4	100	100	0.83	2000	10
5	120	100	0.71	2000	10

2.3. Simulation results

In order to observe the flow field distribution, the cross section through electrode axis and the working fluid nozzle axis are selected as the main cross section. Fig. 2 shows the velocity field of main cross section and the enlarged velocity field of six cross section perpendicular to the electrode axis with a distance of 15 μm between each other. As the machining depth increasing, the flow velocity perpendicular to the electrode axis decreases obviously, which increases the difficulty of debris discharge. In addition, the flow velocity increases gradually from both sides of the electrode surface and the hole inner surface to the middle area.

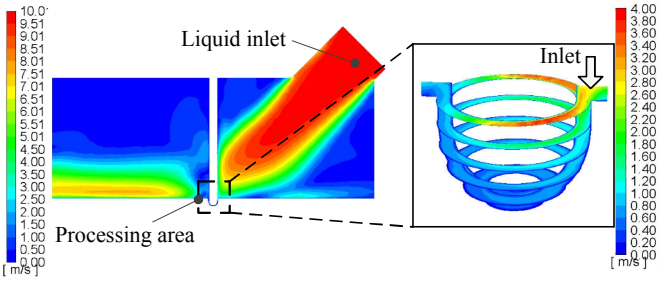

Fig. 2 Velocity field and enlarged velocity field in the gap

Fig. 3 shows the velocity field of the main cross section in the machining gap at different depth-diameter ratios. It could be seen that the flushing effect all deteriorates as the micro-hole depth increases under different depth-diameter ratios. When the micro-hole depth reaches a certain value, the flow velocity is too small that it is difficult to observe its change. As shown in Fig. 3 (e), 14 sampling points are uniformly selected from point A to point B, so that the flow velocity in low flow velocity region is more intuitive.

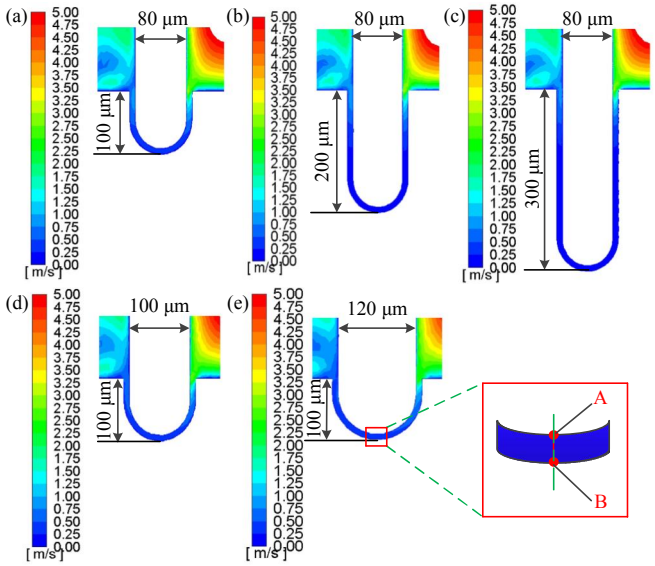

Fig. 3 Velocity field of the main cross section in the machining gap under different depth-diameter ratios. (a) Group 1; (b) Group 2; (c) Group 3; (d) Group 4; (e) Group 5

The flow velocity at each sampling point under different depth-diameter ratios is shown in Fig. 4. The flow velocity at the sampling points in the middle of points A and B is higher than the points on both sides. This is due to the viscosity of the flowing fluid and the friction between the fluid and the channel wall, which makes the velocity of the fluid particle near the channel wall lower and the velocity of the fluid particle in the middle of the channel relatively higher. As shown in Fig. 4 (a), with the tool electrode diameter d remained constant of 80 μm, the flow velocity of the intermediate point decreases sharply from 35 mm/s as the machining depth increases, and was almost zero when the machining depth is 300 μm. As could be seen from Fig. 4 (b), with tool electrode diameter increasing, the flow velocity of the sampling points increases while the machining depth h remained constant of 100 μm. Furthermore, the flow velocity shown in Fig. 4 (b) is in the same order of

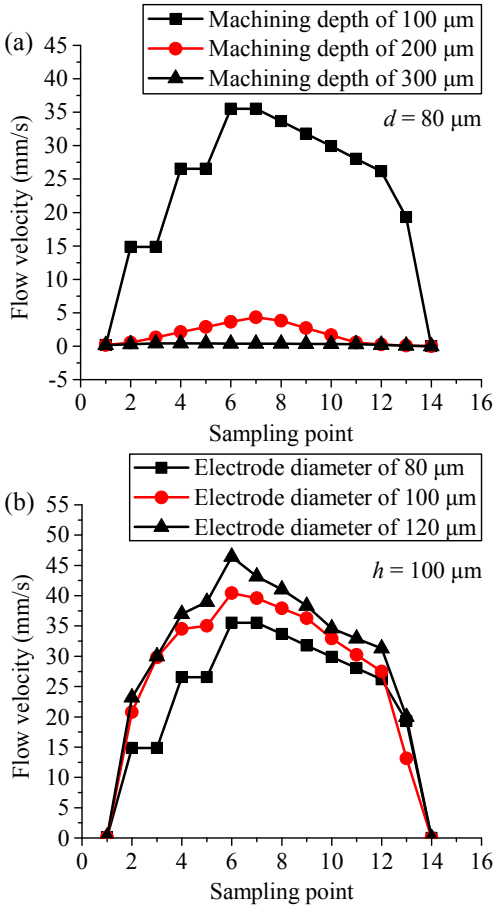

Fig. 4 Flow velocity at each sampling point under different depth-diameter ratios. (a) In the case of different machining depths with electrode diameter of 80 μm; (b) In the case of different tool electrode diameters with machining depth of 100 μm

magnitude as that in Fig. 4 (a), but the variation of velocity is relatively small.

The flow velocity simulation analysis results show that it is difficult for the working fluid to enter the machining gap using external flushing method when the machining depth increases from 50 μm to 200 μm or more with fixed electrode diameter. The debris concentration in machining gap increases accordingly with the flushing effect deteriorates, which will lead to abnormal discharge such as secondary discharge and arc discharge. The degree of electrode wear and workpiece surface burn increases with the frequent occurrence of abnormal discharge, thus affecting the machining accuracy and quality of micro-hole array. When the electrode diameter increases and the machining depth remains unchanged, the flow effect of the working fluid in the machining gap decreases accordingly, and the electrode wear is also intensified due to the same reasons mentioned above. In addition, the machining depth has a greater impact on the flow velocity of working fluid than the electrode diameter, that is, it will have a greater impact on the electrode wear.

3. Experimental procedure

3.1. Experimental system

Fig. 5 (a) shows a schematic diagram of the self-developed precision micro-EDM experimental system. This system consisted of an X–Y–Z–C movement stage, a dielectric fluid recycling system, a pulse power supply system and an image viewing system. During micro-EDM, the movement of the tool electrode is controlled by a computer. The rotating velocity of the tool electrode is controlled by a rotary motor. The dielectric fluid is pumped out, and injectes into the processing part through a needle. The power supply is a multimode micro-energy pulse power supply, including transistor-capacitance (TC) mode, resistance-capacitor (RC) mode and transistor-resistance (TR) mode, which could be switched to meet different machining requirements. The workpiece is connected to the positive electrode of the power supply, and the tool electrode is connected to the negative electrode by a conducting ring. In the image viewing system, the tool electrode tip morphology could be collected and sent to the computer in real time by a CCD camera set on the movement stage. The machined sample is shown in Fig. 5 (b).

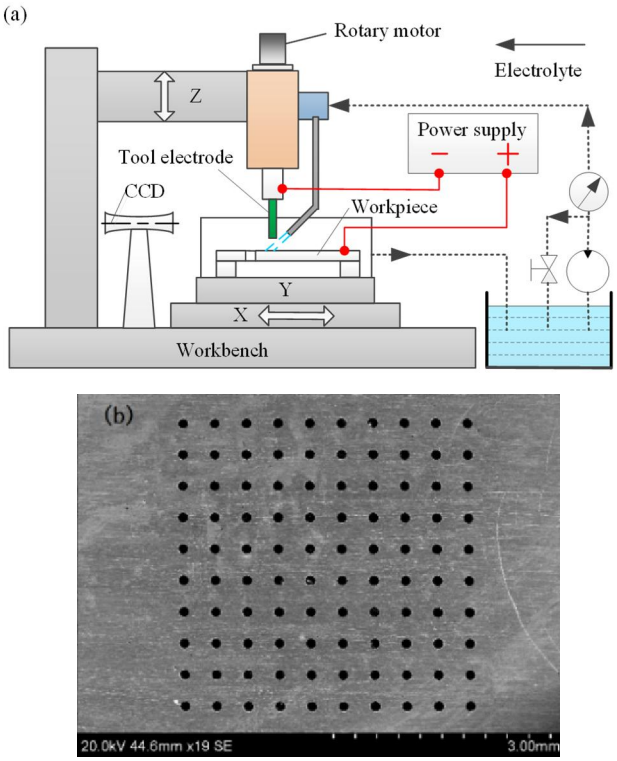

Fig. 5 (a) Schematic diagram of the Micro-EDM system; (b) Sample

3.2. Experimental parameters

In order to get the characteristics of electrode wear and verify the influence of flow field distribution in the machining gap on the electrode wear, the depth-diameter ratio, the electrode rotating velocity, and the outlet velocity of working fluid are selected according to the Table 1. The remaining machining conditions are listed in Table 2.

Table 2. Machining conditions.

Parameter	Value
Workpiece material	Stainless steel
Dielectric fluid	Deionized water
Power mode	TR
Applied voltage (V)	70

3.3. Results

Fig. 6 shows the tool electrode wear when the electrode diameter is 80 μm and the machining depth is 100 μm. In the initial stage (0-10 holes), the electrode has a flat end. With the number of holes machining increasing, the electrode wear begins to appear. The wear in the radial direction of the electrode is greater than that in the axial direction, which indicates that the spark discharge at this stage is mainly concentrated at the radial tip of the electrode.

This is due to the fact that, when a voltage is applied between the tool electrode and the workpiece, the tip of the larger curvature is more likely to accumulate a large amount of charges, causing the dielectric breakdown. In the stage of 10-20 holes, the tool electrode tip gradually evolves into an arc shape, and the axial wear of the electrode starts to be greater than the radial wear of the electrode. In the stage of 20 - 40 holes, the tool electrode tip morphology gradually stabilizes, indicating that the electrode mainly produced axial wear. In the stage of 40 - 80 holes, the tool electrode wear tends to be uniform. The reason is that the morphology of the electrode end face has reached a relatively stable state at this stage, and the discharge probability of each region on the end face tends to be consistent. This phenomenon also appears in several other groups of experiments.

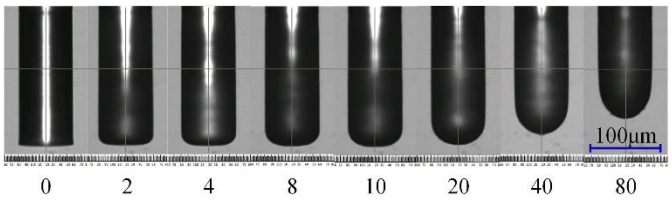

Fig. 6 The tool electrode profile with the increase of the number of machined holes (Group 1)

Fig. 7 shows the axial wear profile of the tool electrode under different depth-diameter ratios. With the increase of the number of machined holes, the axial wear of the five groups of electrodes increases approximate linearly, indicating that the wear of the electrode gradually stabilizes. In Fig. 7 (a), when the electrode diameter d is 80 μm, the axial wear of the tool electrode sharply increases from 72 μm to 419 μm with the increase of machining depth when 100 holes are machined. According to the simulation results of Fig. 4 (a), when the machining depth increases, the working fluid flow velocity in the processing area drastically slows down, leading to the deterioration of the debris removal effect, which makes the wear of the tool electrode increase sharply. Fig. 7 (a) also shows that the accumulated axial wear of electrode with machining depth of 300 μm is larger than that with machining depth of 200 μm. This is because although the flow velocity at machining depth of 300 μm is very close to that at machining depth of 200 μm, the machining time increases, which will increase the accumulation degree of discharge debris in the gap and the probability of abnormal discharge. However, although the accumulated axial wear becomes larger, the growth amplitude and rate of electrode wear at machining depth of 200 - 300 μm are very close to that at machining depth of 100 - 200 μm, as shown in Fig. 8 (a). In Fig. 7 (b), with the machining depth h of 100 μm, the axial wear fluctuation range of the tool electrode is 48 - 72 μm after 100 holes are machined with the increase of electrode diameter, which is less than the axial wear caused by the change of machining depth. This trend is consistent with the simulation results in Fig. 4 (b), illustrating the effectiveness of flow field simulations.

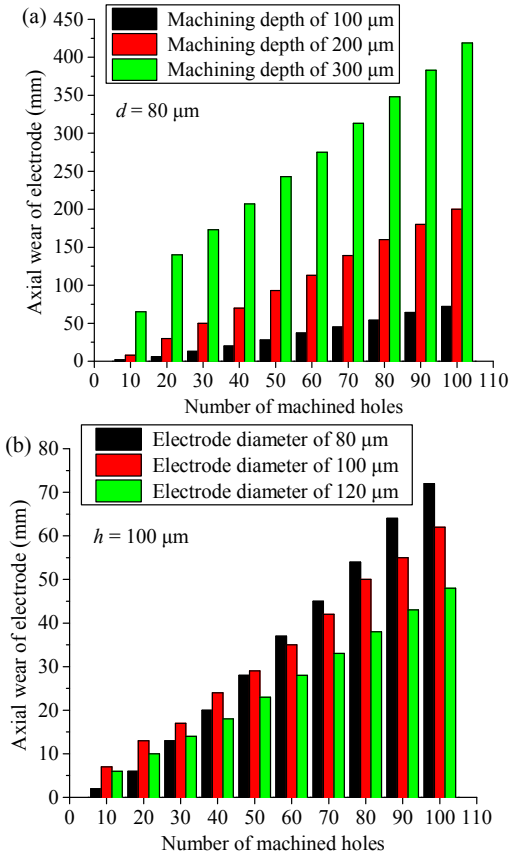

Fig. 7 The axial wear of tool electrode under different depth-diameter ratios. (a) In the case of different machining depths with electrode diameter of 80 μm; (b) In the case of different electrode diameters with machining depth of 100 μm

In Fig. 8, it was assumed that the electrode wear is defined as the average axial wear generated by each hole when the electrode diameter is 80 μm and the machining depth is 100 μm. The actual electrode wear is defined as the average axial wear generated per 100 μm machining depth. As could be seen from Fig. 8 (a), when the machining depth is 0 - 100 μm, 100 - 200 μm, 200 - 300 μm, the electrode wear is 0.8 μm 1.5 μm and 1.4 μm respectively, with an increase rate of 81.0%, which corresponded to the simulation results shown in Fig. 4 (a). The flow velocity is close to zero when the machining depth is 200 μm and 300 μm, which could lead to abnormal discharge such as secondary discharge and arc discharge, resulting in the rapid increase of tool electrode wear. Fig. 8 (b) shows that the range of actual electrode wear is 0.8 μm - 0.5 μm. With the increase of the diameter of the electrode, the reduction of actual electrode wear is 41.2%, which corresponded to the simulation results in Fig. 4 (b) that the flow velocity increases as depth-diameter ratio decreases, which improves the effect of debris removal from the machining gap, thus the wear of the tool electrode decreases.

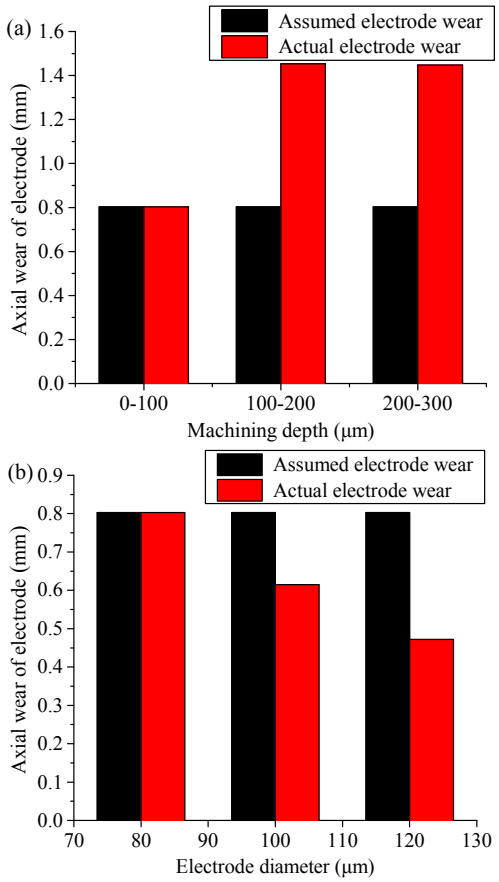

Fig. 8 The comparison chart between actual electrode wear and assumed electrode wear. (a) In the case of different machining depths; (b) In the case of different electrode diameters

In summary, the simulation results of gap flow field could provide a certain basis for the research on the changing trend of electrode wear, and then provide a certain reference for the formulation of electrode wear compensation strategy and the improvement of machining accuracy.

4. Conclusions

In present study, gap flow field simulation analysis under different depth-diameter ratios in micro-EDM is conducted. The experiments on the tip morphology evolution and the wear of tool electrode by changing the parameters of electrode diameter and machining depth are also carried out, and the changing trends of electrode axial wear under different depth-diameter ratios are analyzed from the perspective of the change characteristics of gap flow field.

(1) With depth-diameter ratios increasing in micro-hole array machining, the flow velocity of the working fluid in the machining gap decreases, the flushing effect on the debris is thereby deteriorated. The effect of machining depth on the flow of working fluid in terms of flow velocity in machining gap is more obvious compared with the electrode diameter.

(2) When the number of machined holes is sufficient, the tool electrode wear tends to be uniform, and the morphology of the electrode tip was basically the same. In addition, the axial wear of the tool electrode is approximately proportional to the number of holes that has been machined, indicating that the axial wear of the tool electrode could be compensated evenly.

(3) With the increase of depth-diameter ratios, the axial wear of electrode increases. The results of flow field simulation could show the changing trend of electrode axial wear to some extent. The flushing effect of the working fluid on debris in machining gap is weakened with the depth-diameter ratios increasing, resulting in the occurrence of abnormal discharge. The degree of electrode wear could increase with the frequent occurrence of abnormal discharge.

Acknowledgements

This work is supported by the National Natural Science Foundation of China (No. 51575137), the key project of Natural Science Foundation of Heilongjiang (No. ZD2019E005), and the National Natural Science Foundation of China (No. 51975156).

References

[1] Hourmand M, Sarhan AAD, Sayuti M. Micro-electrode fabrication processes for micro-EDM drilling and milling: a state-of-the-art review. Int J Adv Manuf Tech 2017; 91: 1023-1056.
[2] Ping MM, Li YJ, Wang YL. Fabrication of Micro-Precision Sieves with High Open Area Percentage Using Micro-Electroforming Technology. Adv Mater 2012; 426: 64-68.
[3] Mastud SA, Garg M, Singh R. Recent Developments in the Reverse Micro-Electrical Discharge Machining in the Fabrication of Arrayed Micro-Features. P I Mech Eng C-J Mec 2012; 226: 367-383.
[4] Kitamura T, Kunieda M, Abe K. High-speed imaging of EDM gap phenomena using transparent electrodes. Procedia CIRP 2013; 6: 314-319.
[5] [6] Li G, Natsu W, Yu Z. Study on debris behavior and its influence on EDM characteristics in deep micro-hole machining. Procedia CIRP 2018; 68: 578-581.
[6] Natsu W, Maeda H. Realization of high-speed micro EDM for high-aspect-ratio micro hole with mist nozzle. Procedia CIRP 2018; 68: 575-577.
[7] Ichikawa T, Natsu W. Realization of micro-EDM under ultra-small discharge energy by applying ultrasonic vibration to machining fluid. Procedia CIRP 2013; 6: 326-331.
[8] Zhu GZ, Bai JC, Guo YF, et al. A study of the effects of working fluids on micro-hole arrays in micro-electrical discharge machining. P I Mech Eng B-J Eng. Manuf 2014; 228: 1381-1392.
[9] Wegener K, Kliuev M, Baumgart C. Fluid Dynamics in Electrode Flushing Channel and Electrode-Workpiece Gap During EDM Drilling. Procedia CIRP 2018; 68: 254-259.
[10] Maradia U, Kliuev M, Baumgart C. Efficient machining of complex-shaped seal slots for turbomachinery. CIRP Ann 2018; 67: 209-212.
[11] Bozdana AT, Al-Karkhi NK. Comparative experimental investigation and gap flow simulation in electrical discharge drilling using new electrode geometry. Mech Sci 2017; 8: 289.
[12] Feng G, Yang X, Chi G. Experimental and simulation study on micro hole machining in EDM with high-speed tool electrode rotation. Int J Adv Manuf Tech 2019; 101: 367-375.
[13] Bissacco G, Hansen HN, Tristo G, et al. Feasibility of wear compensation in micro EDM milling based on discharge counting and discharge population characterization. CIRP Ann 2011; 60: 231-234.
[14] Kruth JP, Lauwers WB. Wear Behaviour and Tool Life of Wire-EDM-ed and Ground Carbide Punches. CIRP Ann 2005; 44: 163-166.
[15] Kong DZ, Zhang QH, Fu XZ, et al. Study of electrode wear ratio of piezoelectric self-adaptive micro-EDM. Trans Tech Publ 2014; 589: 505-510.